

The Ω dependence of the velocity divergence distribution

F. Bernardeau¹, R. van de Weygaert², E. Hivon^{3,4} and F. R. Bouchet⁴

¹ *Service de Physique Théorique, C.E. de Saclay, F-91191 Gif-sur-Yvette cédex, France*

² *Kapteyn Astronomical Institute, University of Groningen, P.O. Box 800, 9700 AV Groningen, the Netherlands*

³ *Theoretical Astrophysics Center, Juliane Maries Vej 30, DK-2100 Copenhagen Ø, Denmark.*

⁴ *Institut d’Astrophysique de Paris, CNRS, 98 bis boulevard Arago, F-75014 Paris, France*

5 November 2021

ABSTRACT

Analytical studies based on perturbative theory have shown that the moments of the Probability Distribution Function (PDF) of the local smoothed velocity divergence are expected to have a very specific dependence on the density parameter Ω in the quasi-linear regime. This dependence is particularly interesting as it does not involve the possible bias between the galaxy spatial distribution and the underlying mass distribution. This implies a new and promising method for determining a bias-independent value of Ω based on a reliable determination of the velocity divergence PDF.

In this paper we study the Ω dependence of the velocity divergence PDF and its first moments in a set of N-body simulations, using the so-called Voronoi and Delaunay methods. We show that this dependence is in agreement with the theoretical prediction, even while the number density of velocity field tracers has been diluted to a value comparable to that available in current galaxy catalogues.

In addition, we demonstrate that a sufficiently reliable determination of these statistical quantities is also possible when the measurement of the galaxy peculiar velocities is restricted to the one component along the line-of-sight. Under *ideal*, noise-free circumstances we can successfully discriminate between low and high Ω .

Key words: Cosmology: theory – large-scale structure of the Universe – Methods: numerical – statistical

1 INTRODUCTION

The study of the cosmic velocity field is a very promising and crucial area for the understanding of large-scale structure formation. Since the early work of Rubin et al. (1976) and Burstein et al. (1987) a lot of effort has been invested in the measurement of the large-scale velocity flows (see Dekel 1994 and Strauss & Willick 1995 for recent reviews of the subject). Particularly important for the analysis of these measured velocity fields has been the development of the parameter-free POTENT method by Bertschinger & Dekel (1989). Based on the plausible assumption of potential flow it enabled the construction and study of the full three-dimensional velocity field in a fair fraction of the local Universe out of the measurements of galaxy line-of-sight peculiar velocities. This opened up and triggered a host of studies addressing various issues and aspects of cosmic velocity flows and provided a versatile ground for testing the scenario of large-scale structure formation.

The cosmic velocity field is particularly interesting because of its close and direct relation to the underlying field of mass fluctuations. Indeed, on these large scales the acceleration, and therefore the velocity, of any object is expected to have an exclusively gravitational origin so that it should

be independent of its nature, whether it concerns a dark matter particle or a bright galaxy. Moreover, the linear theory of the generic gravitational instability scenario predicts that at every location in the Universe the local velocity is related to the local acceleration, and hence the local mass density fluctuation field, through the same universal function $f(\Omega) \approx \Omega^{0.6}$ (Peebles 1980). As the linear theory provides a good description on those large scales the use of this straightforward relation implies the possibility of a simple inversion of the measured velocity field into a field that is directly proportional to the field of local mass density fluctuations $\delta = \rho / \langle \rho \rangle - 1$. Such a procedure can be used to infer the value of Ω , through a comparison of the resulting field with the field of mass density fluctuations in the same region. However, the determination of this mass density fluctuation field through the measurement of the local galaxy density fluctuation field, δ_g , may be contrived. The galaxy distribution may be representing a biased view of the underlying mass density fluctuation field. A common and rather simplistic assumption is that δ_g and δ are related via a linear bias factor b ,

$$\delta_g(\mathbf{r}) = b \delta(\mathbf{r}). \quad (1)$$

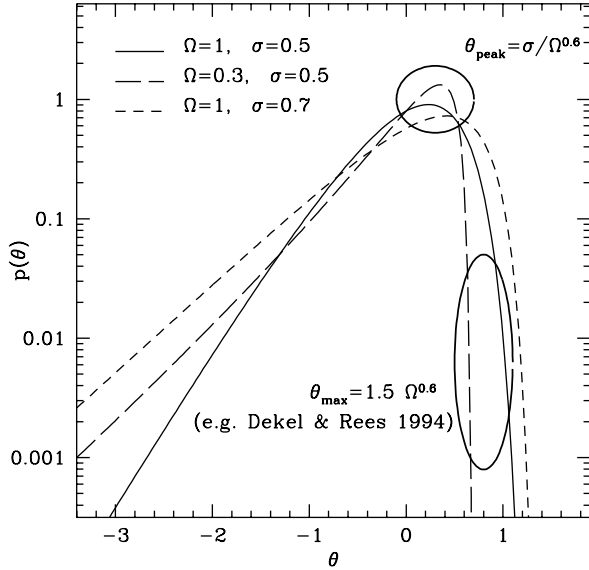


Figure 1. The PDF of the velocity divergence as given by Eq. (10) showing its dependence with Ω and σ .

However, although several physical mechanisms have been invoked to explain such a *linear bias model* (see e.g. Dekel & Rees 1987), by lack of a complete and self-consistent theory of galaxy formation it should as yet only be considered as a numerical factor roughly describing the contrast of galaxy density fluctuations with respect to the mass density fluctuations.

The comparison between the observed local galaxy density fluctuation field and the local cosmic velocity field, invoking equation (1), will therefore provide an estimate of the ratio,

$$\beta = \frac{f(\Omega)}{b} \approx \frac{\Omega^{0.6}}{b}. \quad (2)$$

Various studies, most notably the ones based on a comparison of the galaxy density field inferred from the IRAS redshift survey of Strauss et al. (1990) and the local velocity field reconstructed by the POTENT algorithm (Bertschinger et al. 1990; Dekel, Bertschinger & Faber 1990; see Dekel 1994), have yielded estimates of β in the range $\beta \approx 0.5 - 1.2$ (see Dekel 1994, Strauss & Willick 1995, for compilations of results).

It is then of crucial interest to find ways to disentangle the contribution of Ω and b to β . A variety of methods using *intrinsic* properties of the large-scale velocity field have been proposed to achieve this. One such attempt is based on the reconstruction of the initial density field from the observed distribution of matter through the use of the Zel'dovich approximation. The further assumption of Gaussianity of the initial density probability distribution leads to a constraint on Ω (Nusser & Dekel 1993). Although promising, the quantitative results of this approach may be questionable, as the Zel'dovich approximation provides non-exact results for the induced non-Gaussian properties of the density and velocity field (Bouchet et al 1992, Bernardeau 1994a). Another interesting attempt is the one by Dekel & Rees (1994), who exploit the simple observation that voids have a maximal “emptiness” of $\delta = -1$. On the basis of the corresponding

analysis of the measured velocity field in and around a void region these authors inferred a lower limit on Ω of about 0.3.

In this paper we focus on a method to determine the value of Ω that finds its origin in a statistical analysis of the velocity field. The foundation for this method is formed by analytical work within the context of the perturbation theory for the evolution of density and velocity fluctuations. In particular, it focuses on the statistical properties of the divergence of the locally smoothed velocity field θ , which is defined as

$$\theta \equiv \frac{\nabla \cdot \mathbf{v}}{H}, \quad (3)$$

where \mathbf{v} is the time derivative of the comoving coordinate \mathbf{x} , and $\nabla = \partial/\partial\mathbf{x}$. The method, proposed by Bernardeau (1994a) and Bernardeau et al. (1995), exploits the relations between the lower order moments of the probability distribution function (PDF) of θ , and the explicit dependence on Ω of these relations. The specific form of these relations were derived under the assumption of Gaussian initial conditions.

The viability of the method was demonstrated by Bernardeau et al. (1995), who used the strong Ω -dependence of the skewness factor of θ , or rather the third normalized moment T_3 ,

$$T_3 \equiv \langle \theta^3 \rangle / \langle \theta^2 \rangle^2 \propto \Omega^{-0.6} \quad (4)$$

to estimate successfully the density parameter in N-body simulations of structure formation. A tentative application of this method to the observed velocity field as processed by the POTENT method yielded results consistent with $\Omega = 1$. Moreover, subsequent work by Bernardeau & van de Weygaert (1996) showed that the theoretical predictions concerning the complete overall shape of the PDF of θ were valid. They demonstrated this by comparison of the analytically predicted PDF with the PDF determined from a large CDM N-body simulation with $\Omega = 1$. In order to deal with the major complication of obtaining clean and straightforward numerical estimates of the statistical properties of the velocity divergence field from the discretely sampled velocity field, they developed two new techniques. These techniques exploit the minimum triangulation properties of Voronoi and Delaunay tessellations (Voronoi 1908, Delaunay 1934, see Van de Weygaert 1991, 1994 for references and applications).

A Voronoi tessellation of a set of particles is a space filling network of polyhedral cells, with each cell being defined by one of the particles as its nucleus and delimiting the part of space closer to this nucleus than to any other of the particles. Closely related to the Voronoi tessellation is the Delaunay tessellation, a space filling lattice of tetrahedra (in three dimensions). Each of the tetrahedra in the Delaunay tessellation has four particles of the set as its vertices, such that the corresponding circumscribing sphere does not have any other particle inside. Through the duality relation of the Voronoi and the Delaunay tessellation it is possible to obtain one from the other.

In the method based on the Voronoi tessellation – the “Voronoi method” – the velocity field is defined to be uniform within each Voronoi polyhedron, with the velocity at every location within each cell being equal to that of its nucleus. The obvious implication of such an interpolation scheme is that the only regions of space where the velocity divergence, as well as the shear and vorticity, acquires a non-

zero value is in the polygonal walls that separate the cells. While the Voronoi method can be regarded as a zeroth order interpolation scheme, yielding a discontinuous velocity field, the ‘‘Delaunay method’’ can be seen as the corresponding first order scheme. Basically it constructs the velocity field within each Delaunay tetrahedron through linear interpolation between the velocities of the four defining particles. Evidently, the velocity field constructed by the Delaunay method is a field of uniform velocity field gradients within each Delaunay cell. In the following we consider the statistical properties of the local velocity divergence when it is filtered by a top-hat window function following a *volume weighting* prescription. In practice the local filtered divergence is computed on 50^3 grid points in all cases. Depending on the method used to define the velocity field, the filtered divergence is given by a sum of intersections of a sphere with either planar polygonal walls or tetrahedra (each of them being multiplied by the local divergence) divided by the volume of the sphere. In such a volume weighting scheme the filtered quantities do not depend on the local number density of tracers. But of course the more numerous they are, the more accurately determined are the local divergences. For an extensive description and preliminary tests of the two techniques we refer to Bernardeau & van de Weygaert (1996).

With the intention of demonstrating the potential and practical applicability of our method, this paper presents the results of a systematic study of the Ω dependence of the moments and the PDF of the velocity divergence θ in N-body simulations of structure formation, using the numerical schemes of the Voronoi and the Delaunay method. To this end, we will first recall the relevant theoretical results on the statistical properties of θ in Section 2, thereby underlining the main features of importance to our study. This theoretical groundwork is followed by Section 3, containing the presentation of the numerical results of the statistical analysis of PM N-body simulations of structure formation in $\Omega = 1$ and $\Omega < 1$ universes. While the first subsection, § 3.1, concerns the statistical quantities that were determined in a very large sample and thus with maximum attainable accuracy, the second subsection § 3.2 is devoted to the issue to what extent these results get affected when the sample is strongly diluted. The latter is particularly important as we are interested in the reliability of our method for samples with a number density comparable to that of available galaxy catalogues. Also of immediate relevance for a practical application is the question of how far the results of the statistical analysis get influenced when the velocity of the particles in the sample are known along only one direction. This issue, of crucial importance within the context of the statistical analysis of observational catalogues, is treated in a third subsection, in § 3.3. Finally, following the successful application of our method under the circumstances described above, we conclude with a summary and a discussion of possible complications and prospects for our statistical method to infer a bias-independent value of Ω .

2 PERTURBATION THEORY OF STRUCTURE FORMATION AND THE VELOCITY FIELD PROBABILITY DISTRIBUTION FUNCTION

Perturbation Theory (PT) is extremely useful for the study and analytical description of the mildly non linear evolution of density and velocity fields. In particular within the context of structure forming out of Gaussian initial conditions perturbation theory has been extensively developed in a large body of work (see e.g. Bernardeau 1994a,b). In the case of these Gaussian initial conditions the complete set of moments of the smoothed velocity and density fields can be computed analytically, in particular if these fields are top-hat filtered. The corresponding PDF can be computed through re-summation of the series of moments.

One of the most straightforward and useful results in the context of perturbation theory is the relation between the third moment $\langle \theta^3 \rangle$ and the second moment $\langle \theta^2 \rangle$ of the probability distribution function of θ ,

$$\langle \theta^3 \rangle = T_3 \langle \theta^2 \rangle^2 = T_3 \sigma_\theta^4. \quad (5)$$

The coefficient T_3 depends on the cosmological parameter Ω , on the shape of the power spectrum, on the geometry of the window function that has been used to filter the velocity field and even on the value of the cosmological constant Λ , although the latter is an almost negligible weak dependence. In fact, the dependence of T_3 on Ω is substantially stronger than the one of the equivalent coefficient for density field. For instance, for a top-hat window function and a power law initial power spectrum of index n , i.e.

$$P(k) \equiv \langle \delta(\mathbf{k})^2 \rangle \propto \langle \theta(\mathbf{k})^2 \rangle \propto k^n, \quad (6)$$

one obtains the following expression for T_3 ,

$$T_3 = \frac{-1}{\Omega^{0.6}} \left[\frac{26}{7} - (3 + n) \right]. \quad (7)$$

As T_3 can be directly determined from observations, one can use its strong dependence on Ω to obtain an estimate of Ω , as has been done by Bernardeau et al. (1995).

More generally, Perturbation Theory enables one to infer the whole set of the cumulants $\langle \theta^p \rangle$ to their leading order. All of them are related to the second moment via the relation

$$\langle \theta^p \rangle = T_p \langle \theta^2 \rangle^{p-1}, \quad (8)$$

and as in the case of T_3 all the coefficients T_p possess a strong dependence on the value of Ω (Bernardeau 1994b). To a good approximation, this dependence on cosmological parameters can be written as

$$T_p(\Omega, \Lambda) \approx \frac{1}{\Omega^{(p-2)0.6}} T_p(\Omega = 1, \Lambda = 0). \quad (9)$$

This property, given here for the moments, naturally extends itself to the shape of the complete velocity divergence PDF $p(\theta)$. This can be directly appreciated from the work by Bernardeau (1994b), who showed that the PDF can be calculated from its moments T_p and the value of σ_θ^2 through a Laplace transform of its generating function φ_θ

$$p(\Omega, \theta) d\theta = \int_{-\infty}^{+\infty} \frac{dy}{2\pi i \sigma_\theta^2} \exp \left[-\frac{\varphi_\theta(\Omega, y)}{\sigma_\theta^2} + \frac{y\theta}{\sigma_\theta^2} \right] d\theta. \quad (10)$$

The moment generating function $\varphi_\theta(\Omega, y)$, given by

$$\varphi_\theta(\Omega, y) = \sum_{p=2}^{\infty} -T_p(\Omega) \frac{(-y)^p}{p!}, \quad (11)$$

can be related to the spherical collapse dynamics in the cosmology under consideration (see Appendix A). Although this calculation is almost intractable in the general case, it has been shown that at least in one particular case one can evaluate this expression analytically. In the specific case of a power law density perturbation spectrum with an index $n = -1$ in combination with a top-hat smoothing, it is possible to invoke some approximations that enable the derivation of a simple analytic fit for the PDF $p(\theta)^*$ (see Appendix A). This fit is given by

$$p(\theta)d\theta = \frac{([2\kappa - 1]/\kappa^{1/2} + [\lambda - 1]/\lambda^{1/2})^{-3/2}}{\kappa^{3/4}(2\pi)^{1/2}\sigma_\theta} \times \exp\left[-\frac{\theta^2}{2\lambda\sigma_\theta^2}\right] d\theta, \quad (12)$$

with $\kappa = 1 + \theta^2/(9\lambda\Omega^{1.2})$, and $\lambda = 1 - 2\theta/(3\Omega^{0.6})$.

The behaviour of this function $p(\theta)$ has been illustrated in figure 1 for various values of Ω and σ_θ . Qualitatively, one can see that the dependence of the shape on Ω reveals itself in two ways: (1) the location of its cut-off at high positive values of θ and (2) the location of its peak.

As for (1), the maximum value that θ can obtain is known exactly and is not dependent on the approximations that have been invoked to derive expression (12)

$$\theta_{\max} = 1.5 \Omega^{0.6}. \quad (13)$$

The value of θ_{\max} determines the location of the cut-off, and therefore the maximum expansion rate in voids. The value of 1.5 is the difference in value of the Hubble parameter in an empty, $\Omega = 0$, Universe and that of an Einstein-de Sitter Universe, $\Omega = 1$. Evidently, this is reflecting the fact that the interior of the deepest voids locally mimic the behaviour of an $\Omega = 0$ Universe. Recall that the suggestion by Dekel & Rees (1994) of using the maximum emptiness of voids to constrain Ω is also based on a similar feature.

Also quite sensitive to the value of Ω are the position of the peak of the distribution function $p(\theta)$, i.e. the most likely value of θ , and the overall shape of $p(\theta)$. Using the Edgeworth expansion (Juszkiewicz et al. 1995, Bernardeau & Kofman 1995) one can show that the value of θ for which the distribution reaches its maximum is given by

$$\theta_{\text{peak}} \approx -\frac{T_3}{2} \sigma_\theta = \frac{1}{\Omega^{0.6}} \sigma_\theta. \quad (14)$$

In fact, a procedure exploiting this dependence of shape and peak location of $p(\theta)$ will probably yield a more robust measure of Ω than the maximum value of θ_{\max} as it will be less bothered by the noise in the tails.

3 THE Ω DEPENDENCE IN NUMERICAL SIMULATIONS

By means of numerical simulations we have investigated the discussed dependence of the PDF of θ . These N-body sim-

ulations use a Particle-Mesh (PM) code (Moutarde et al. 1991) with a 256^3 grid to follow the evolution of a system of 256^3 particles. For our project we used two simulations, one with Ω having a value of $\Omega = 1$ and the second one of $\Omega < 1$. By analyzing the latter at different time-steps we explore situations for different values of Ω . The particle distribution in the two simulations corresponds to a density and velocity fluctuation field with a $P(k) \propto k^{-1}$ spectrum.

As can be seen in Table 1, the variances σ_θ do not differ significantly for the different values of Ω for a given filtering radius. The fact that the values of the variance are comparable simplifies a comparison of the PDF substantially, which makes the interpretation in terms of the intrinsic Ω dependence more straightforward.

3.1 Measurements with a large number of tracers

The first step of our analysis concerns an exploration of the velocity field using a large number of tracers. For this study the number of selected particles in each simulation is about 70,000, which for a cell radius of about 6% of the box size leads to a mean number of 67 particles per cell. The selection procedure used here is deliberately biased towards low-density regions by inducing it to retain a uniform density of particles all over the simulation box. Except for its goal of achieving a better velocity field coverage of low-density regions such a selection bias is not expected to influence the velocity field analysis.

The methods that we use to analyze the simulations are exactly the same ones as described by Bernardeau & van de Weygaert (1996). In fact, at this stage we only used the Delaunay method to calculate numerically the shape of the PDF of the velocity divergence. The results for the case of a large number of velocity field tracers are shown in Fig. 2. The results are in good agreement with the theoretical predictions for the values of T_3 and T_4 (see Table 1), as well as with the theoretical shape of the PDF (Fig. 1).

It is in particular worth noting that the specific features expected from equation (12) are indeed confirmed by the numerical results. Notably, the locations of the cut-off, which are very sensitive to rare event discrepancies, are well reproduced (solid and dotted lines). Moreover, as can be observed from the insets, also the position and shape of the peak have been reproduced very well (solid lines), providing a strong discriminatory tool between different values of Ω .

Within the context of these observations, we should issue a few side remarks. Although the shape (12) is very attractive because it is a close analytic form, one should have in mind that it is only approximate. Indeed it is derived from an approximate expression for the cumulant generating function. The differences do not reveal for the overall shape (the logarithmic plots) but are significant for the shape of the peaks. For calculating the theoretical predictions we are then forced to use a more accurate description of the cumulants. To achieve this we use the relations (A.13, A.14) with $n = -0.7$ (the expression 12 corresponds to $n = -1$) in the integral (A.15) which is then computed numerically. It is still an approximate expression, but it yields the correct value for T_3 and a very good approximation for the higher order cumulants. We should emphasize that this slight modification is only instrumental in obtaining the correct shape of the PDF around its maximum, which is indeed almost

* This fit is obtained through approximations which tend to lower the values of the moments (appendix A). The PDF (12) presented here is actually more accurate if $n \approx -1.3$.

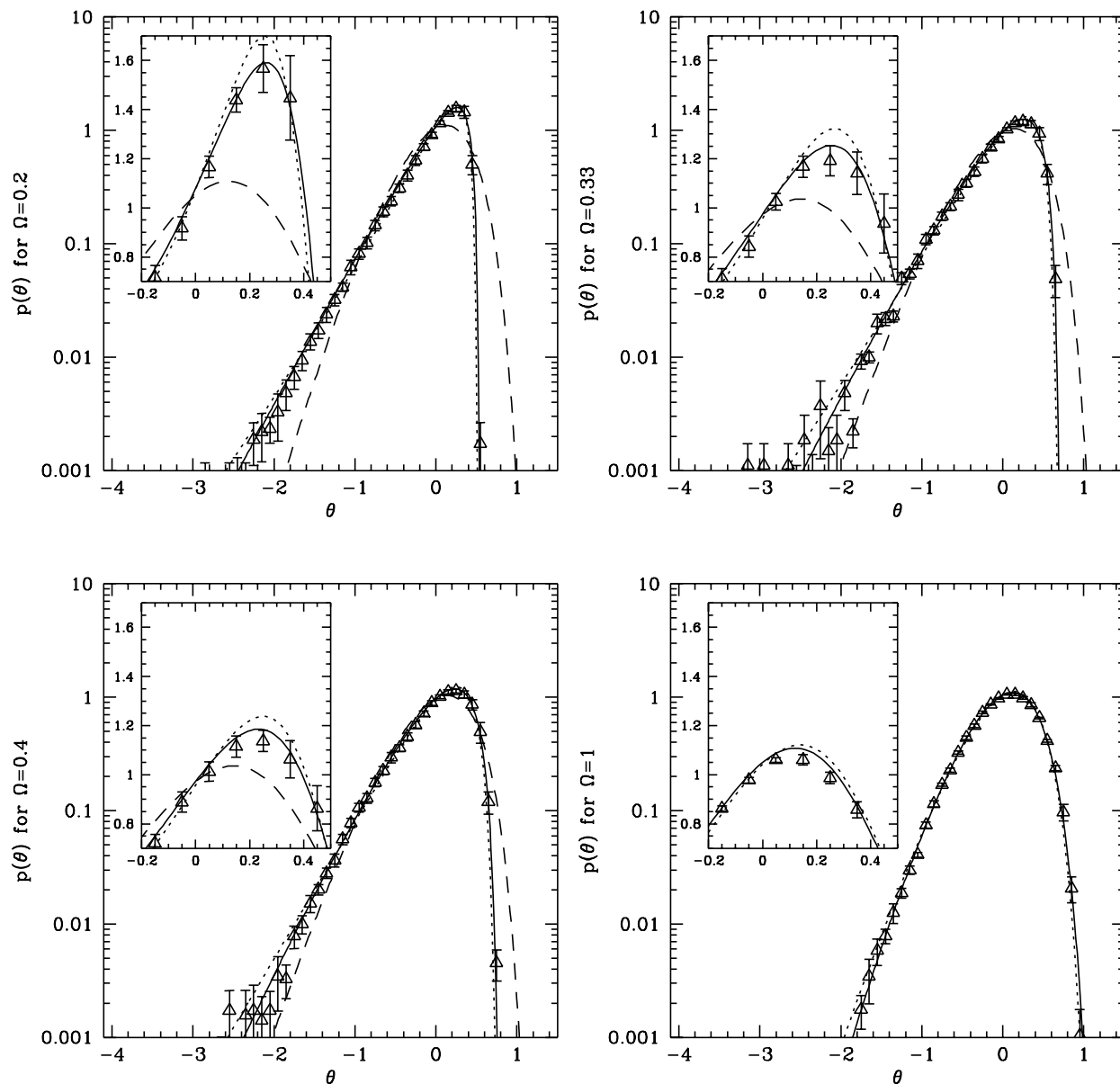


Figure 2. The PDF of the velocity divergence for various values of Ω . The dotted lines correspond to the approximate analytic fit (Eq.12) and the solid lines to the theoretical predictions using (A.15) and (A.14) with $n = -0.7$ obtained for the measured values of σ and Ω . The dashed lines are the predictions for $\Omega = 1$ and the same variance. The numerical estimations have been obtained using the Delaunay method.

entirely determined by the values of the low order moments. This may be understood for example from the properties of the Edgeworth expansion, for which we refer to Juszkiewicz et al. 1995 and Bernardeau & Kofman 1995.

3.2 The effects of dilution

In order to check the robustness of the results when only a limited number of tracers for the velocity field is available, we performed numerical experiments where only 10,000 particles are used to trace the velocity field. The selection of the sample points in this diluted sample is completely random and does not invoke the specific biased selection procedure

that was used in the case described in the former subsection. For this case of diluted samples, we used both the Delaunay and the Voronoi methods for analysis.

Figure 3 shows the PDFs obtained with both methods, for an $\Omega = 1$ simulation and for an $\Omega = 0.33$ simulation. Both the Voronoi and the Delaunay methods appear to yield numerical results that are in reasonably good agreement with the predicted PDF. Particularly encouraging is the result born out by the insets, namely the fact that the shape of the peak can still be used as a strong discriminatory tool between different values of Ω .

Investigating Fig. 3 in somewhat more detail, we can observe that the results obtained by the two methods are af-

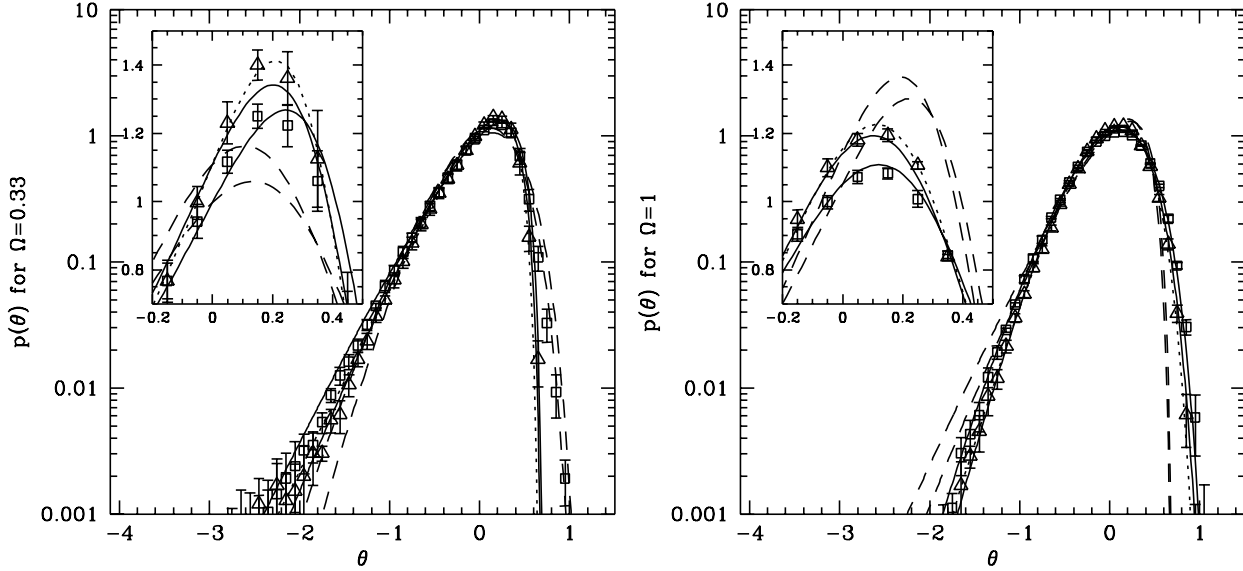


Figure 3. Effects of dilution for $\Omega = 0.33$ (left panels) and $\Omega = 1$ (right panels). The PDF-s have been obtained with only 10,000 tracers in total which gives an average of about 10 particles per cell. The squares show the results of the Voronoi method and the triangles the results of the Delaunay method. The solid lines correspond to the theoretical predictions for the variance obtained with each method and the “right” assumption for Ω and the dashed line with the “wrong” assumption for each case and method.

ected somewhat differently by the dilution procedure. The PDFs obtained with the Voronoi method generally possess a less sharply defined tail at the side of the high θ values. This effect appears to be stronger for the low Ω case. This behaviour may originate in the fact that the divergence is localized to a limited part of space, non-zero values being confined to the walls of the tessellation. In such a situation Poisson like errors in the measurements are expected to become particularly prominent in the heavily diluted areas of the void regions. An additional difference is a slight underestimation of the values of the T_p coefficients by the Voronoi method (see Table 1). Unfortunately, we do not see a possibility to correct for such effects. On the other hand, the Delaunay method seems to be more robust against such effects. However, it tends to underestimate the value of the variance and the higher order moments. The latter is probably a consequence of the fact that the effective filtering radius tends to be larger.

3.3 The effects of reducing the information to one velocity component

A major complication in the analysis of velocity fields under practical circumstances is the fact that only the velocity component along the line of sight can be measured. This therefore forms the second issue that we address in this paper.

As yet we restrict ourselves to an artificial situation with ideal measurements, not yet to investigate the determination of the statistical quantities associated with the velocity field under realistic circumstances. To simplify furthermore our investigations we assume that we can use the approximation of an infinitely remote observer so that the radial velocity can be identified with one velocity component, namely the x -direction in the following. More specifically, we address the effects of the reduction of information concerning the veloc-

ity field traced by a diluted sample of points. In principle, the fact that the velocity field is only known along one direction should not pose any problem. In the usual structure formation scenarios based on gravitational instability the large scale velocity field is expected to be non-rotational, implying it to be a potential flow and therefore the gradient of a potential that can be inferred from the measurement of only one component of the velocity (Bertschinger et al. 1990, Dekel et al. 1990).

In the Voronoi method non-zero values of the divergence θ are restricted to the walls of the Voronoi tessellation, where the local divergence is given by

$$\theta_{\text{wall}} = \mathbf{n} \cdot \Delta \mathbf{v}, \quad (15)$$

with \mathbf{n} being the normed vector orthogonal to the wall and $\Delta \mathbf{v}$ the difference of the velocities on the opposite sides of the Voronoi wall. The expression for the local vorticity is given by

$$\omega_{\text{wall}} = \mathbf{n} \times \Delta \mathbf{v}. \quad (16)$$

Assuming potential flow, and hence a zero value of ω , this implies relations between the various components of $\Delta \mathbf{v}$ and the following expressions for θ_{wall} :

$$\theta_{\text{wall}} = \frac{\Delta v_x}{n_x} = \frac{\Delta v_y}{n_y} = \frac{\Delta v_z}{n_z}. \quad (17)$$

In practice, this introduces the numerically unstable operation of dividing by one component \mathbf{n} as it can be arbitrarily close to zero. It may therefore be more reasonable to try to estimate the value of θ_{wall} using the stable, but ad-hoc, prescription of

$$\theta_{\text{wall}}^{\text{estim.}} = \Delta v_x \frac{n_x}{n_x^2 + \epsilon}, \quad (18)$$

where ϵ is a small parameter of the order of $\epsilon \approx 0.1$.

Note that such a prescription is not self-consistent in

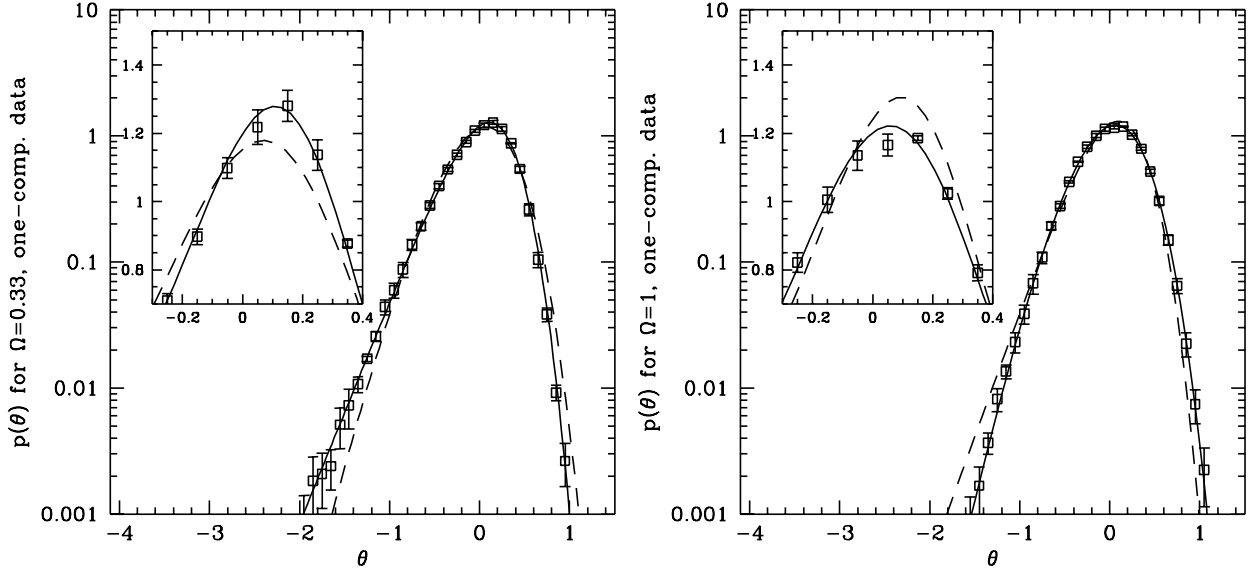


Figure 4. Effects of reduction of the information on the velocity field to only one component for $\Omega = 0.33$ (left panel) and $\Omega = 1$ (right panel). We used the estimator (18) with $\epsilon = 0.1$ to determine numerically the local divergences. The solid lines correspond to the model (21) obtained from (19) with the parameters μ and σ_e given in Table 2. The dashed lines are the resulting shapes of the PDF-s when one uses the same parameters but the “wrong” value for Ω (1 instead of 0.33 in the left panel, 0.33 instead of 1 in the right one).

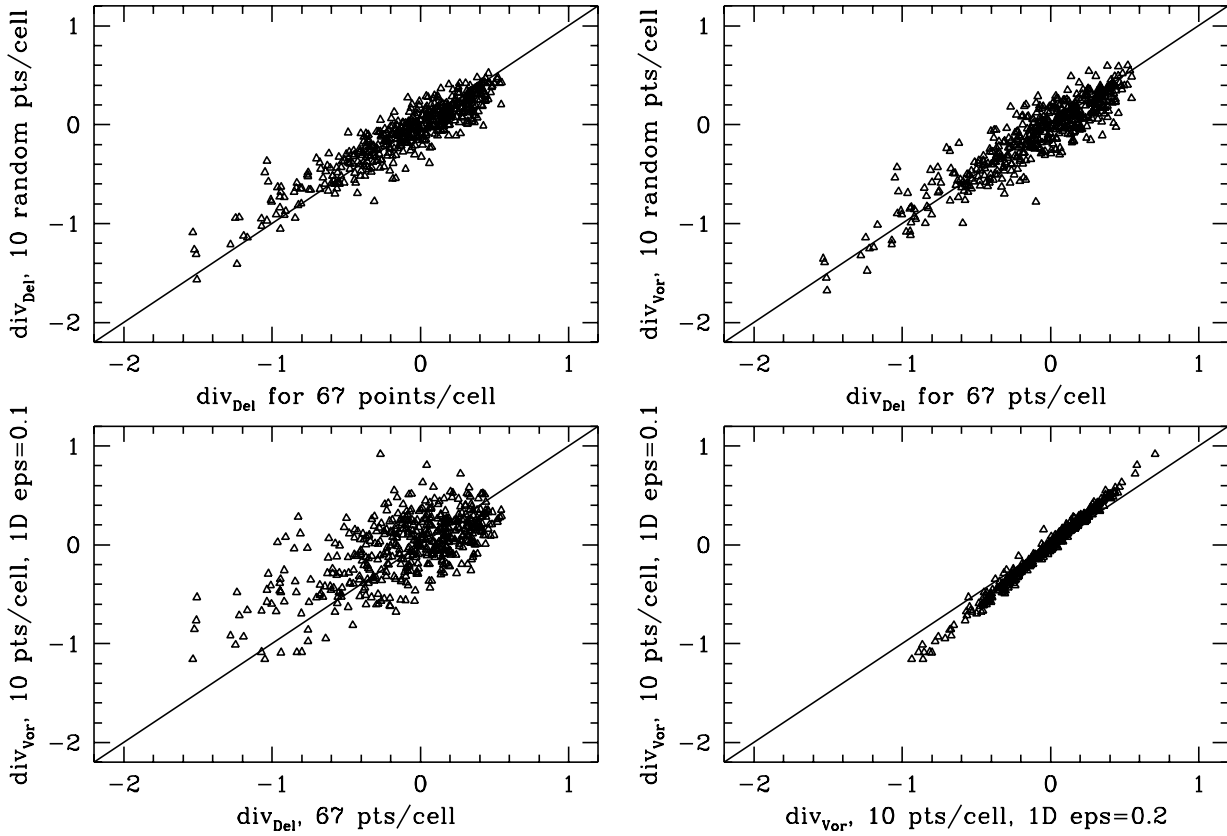


Figure 5. Scatter plots that show the differences of the various estimators of the local divergence measured at 500 different random locations.

reproducing the full 3D velocity field.[†] Indeed, depending on the way one goes from cell A to cell B – and there are infinitely many ways to go from A to B, even while they are direct neighbours – one will not necessarily find the same value for $\theta_{\text{wall}}^{\text{estim}}$ using the equivalent prescriptions for Δv_y or Δv_z . The method that we adopt here will therefore certainly not be the most accurate method. However, we may expect it to be a reasonable approximation, and will therefore use it here to illustrate the properties in which we are interested.

Figure 4 displays the results obtained with (18) for $\epsilon = 0.1$. Evidently, the results get affected to quite some extent by the transition from (15) to (18). This leads to the key question whether it is still feasible to reliably recover the statistical information on θ or not. As can be observed from the scatter plots in Fig. 5, the change from a situation in which one has knowledge of the full velocity to one where this has been limited to only one component thereof introduces a large scatter. However, we found that it is possible to define a meaningful representation of the scatter plots in terms of the following empirical description:

$$\theta_{\text{estim.}} = \mu (\theta + e). \quad (19)$$

Within this expression the coefficient μ is a constant with some fixed value. The scatter is represented by the quantity e , a Gaussian random variable whose value is *independent* of θ and which has a vanishing mean. Using the measured values of the variance and the skewness of the distribution it is possible to estimate the value of μ and the value of the rms fluctuation σ_e of e . From (19) one can readily infer that

$$\begin{aligned} \sigma_{\text{estim.}} &= \mu \sqrt{\sigma_\theta^2 + \sigma_e^2} \\ T_3 \text{ estim.} &= \frac{\sigma_\theta^4}{\mu (\sigma_\theta^2 + \sigma_e^2)^2} T_3 \end{aligned} \quad (20)$$

where σ_θ is the exact rms fluctuations of θ and T_3 its third cumulant, while $\sigma_{\text{estim.}}$ and $T_3 \text{ estim.}$ are the corresponding estimated values. By solving this set of equations one can find the values of μ and σ_e . Their values for various Ω and ϵ are listed in Table 2.

Moreover, significant within the context of the ultimate goal of developing an unbiased estimator of Ω , is that these parameters were found to be almost independent of the value of Ω . More specifically, it turns out that the value of μ only depends on the adopted value of ϵ , whereas σ_e is independent of Ω and only marginally dependent on ϵ . This can clearly be appreciated from the bottom right-hand panel of Fig. 5, which demonstrates that the two estimations of θ , one based on $\epsilon = 0.1$ and the other on $\epsilon = 0.2$, are basically proportional to each other. It may therefore be argued that it is quite natural to expect that the noise e introduced by this method is somehow intrinsic to the distribution.

In Appendix B we describe an extremely simple model based on the assumption that the relative velocity of two

[†] This can be readily appreciated from the fact that the normal \mathbf{n} to a wall in the Voronoi tessellation is proportional to the vector $\Delta \mathbf{r}$ between the two points on each side of the wall. Thus, if it were possible to build a consistent velocity field from the constraints (17) it would imply $\Delta \mathbf{v} \propto \Delta \mathbf{r}$ yielding not only a vanishing vorticity but also a vanishing shear.

Table 2. Numerical values of the parameters μ (bias) and σ_e (noise) introduced by the calculation (18) of the velocity divergence.

| $\Omega = 0.33$ | $\epsilon = 0.1$ | $\epsilon = 0.2$ |
|-----------------|------------------|------------------|
| μ | 0.73 | 0.56 |
| σ_e | 0.25 | 0.27 |
| $\Omega = 1$ | $\epsilon = 0.1$ | $\epsilon = 0.2$ |
| μ | 0.75 | 0.57 |
| σ_e | 0.24 | 0.26 |

Table 3. Analytical estimations of the parameters μ and σ_e (see Appendix B).

| $\Omega = 0.33$ | $\epsilon = 0.1$ | $\epsilon = 0.2$ |
|-------------------------------------|------------------|------------------|
| $\mu(\epsilon)$ | 0.60 | 0.49 |
| $\sigma_e(\epsilon, \sigma_\theta)$ | 0.20 | 0.23 |
| $\Omega = 1$ | $\epsilon = 0.1$ | $\epsilon = 0.2$ |
| $\mu(\epsilon)$ | 0.60 | 0.49 |
| $\sigma_e(\epsilon, \sigma_\theta)$ | 0.19 | 0.22 |

particles is proportional to their relative position. This allows us to compute analytically the parameters μ and σ_e entailed by the use of the numerical scheme (18). One can show that they are both independent on Ω , and only depend on ϵ and σ_θ , with $\sigma_e < \sigma_\theta$. These analytical predictions are listed in Table 3. They appear to be fairly close to their numerical measurements. The discrepancy between the analytical and numerical estimations of these parameters is due to the loss of information associated with the projection of the velocity from three to one dimensions. Although this is not fairly represented by our model, the discrepancy seems to be quite small.

On the basis of the simple model described in Eq. (19) it is possible to reconstruct the corresponding shape of the distribution of $\theta_{\text{estim.}}$,

$$p_{\text{estim.}}(\theta_{\text{estim.}}) = \int_{-\infty}^{+\infty} p\left(\frac{\theta_{\text{estim.}}}{\mu} - e\right) \frac{\exp(-e^2/2/\sigma_e^2)}{(2\pi)^{1/2}} \frac{de}{\sigma_e} \quad (21)$$

where $p(\theta)$ is given by Eq. (12). A comparison of the resulting distribution (21) with the measured histograms is shown in Fig. 4. The agreement appears to be quite good, rendering this phenomenological description a quite valuable one.

Evidently, we are still able to clearly distinguish between the scenario with a high value of Ω and the ones with a low value, although the distinction is not as clear as in the previous cases based on ideal sampling circumstances. Looking into some detail, we come to the conclusion that the signal has been diluted somehow by the noise e , and that there is a competition between the true rms of the divergence σ_θ and the value of σ_e . In this respect it is also important to note that it is crucial for a successful determination of Ω to have good estimates of both μ and σ_e . Once these parameters have been determined, and as long as $\sigma_\theta > \sigma_e$, we can see no further problem in distinguishing between the different cosmological scenarios. Fig. 4 gives an idea of the magnitude of the discrepancy that one gets when

Table 1. Cumulants from the Perturbation Theory and as estimated by the various numerical methods.

| # tracers per cell | cumulants | $\Omega = 0.2$ | $\Omega = 0.33$ | $\Omega = 0.4$ | $\Omega = 1$ |
|-----------------------------|-----------------------|-----------------|------------------|-----------------|------------------|
| ∞ | T_3^{PT} | -4.5 | -3.33 | -2.97 | -1.71 |
| Perturbation Theory | T_4^{PT} | 31.41 | 17.22 | 13.67 | 4.55 |
| ≈ 65 | σ^{Del} | 0.37 ± 0.01 | 0.41 ± 0.01 | 0.42 ± 0.01 | 0.38 ± 0.005 |
| Delaunay Method | T_3^{Del} | -4.52 ± 0.2 | -3.3 ± 0.2 | -2.9 ± 0.2 | -1.54 ± 0.1 |
| | T_4^{Del} | 31.5 ± 2.5 | 17.3 ± 3 | 12.8 ± 2.5 | 3.1 ± 0.7 |
| ≈ 10 | σ^{Del} | – | 0.36 ± 0.01 | – | 0.35 ± 0.005 |
| Delaunay Method | T_3^{Del} | – | -3.8 ± 0.2 | – | -1.84 ± 0.1 |
| | T_4^{Del} | – | 24.7 ± 3 | – | 5.4 ± 1 |
| ≈ 10 | σ^{Vor} | – | 0.40 ± 0.01 | – | 0.38 ± 0.003 |
| Voronoi Method | T_3^{Vor} | – | -3.2 ± 0.2 | – | -1.51 ± 0.04 |
| | T_4^{Vor} | – | 19.4 ± 5.5 | – | 3.62 ± 1.5 |
| ≈ 10 | σ^{Vor} | – | 0.35 ± 0.006 | – | 0.34 ± 0.009 |
| one velocity | T_3^{Vor} | – | -2.40 ± 0.3 | – | -1.14 ± 0.07 |
| component, $\epsilon = 0.1$ | T_4^{Vor} | – | 11.9 ± 4 | – | 2.9 ± 2.3 |

one assumes a wrong value of Ω . In the left panel this concerns the case wherein one take a value of $\Omega = 1$ instead of the actual value of $\Omega = 0.33$, while in the right-hand panel it concerns the reverse situation.

At this point it is worthwhile to stress once more that so far we only tested the method for *ideal* measurements of the line-of-sight velocities. Noise in the measured values of these velocities was not yet taken into account. Moreover, besides the fact that this noise has quite a large value, an evaluation of its influence is substantially complicated as it not only concerns random measurement errors but also contains contributions from a plethora of, partially un-understood, systematic effects. In a work in preparation we will attempt to develop specific techniques for estimating the velocity divergence PDF from such noisy line-of-sight measurements.

4 DISCUSSION AND CONCLUSIONS

We have tested and confirmed the validity of the strong Ω dependence of the Probability Density Function (PDF) of the velocity divergence that had been predicted on the basis of analytical Perturbation Theory calculations. These tests are based on a numerical analysis of N-body simulations of structure formation in a Universe with a Gaussian initial density and velocity fluctuation field. On the basis of this verification we may conclude that the analytical predictions of Perturbation Theory yield very accurate results for a wide range of cosmological models.

The main practical implication of our work is the basis it offers for a potentially very valuable and promising estimator of the value of Ω , an estimator independent of a possible bias between the distribution of galaxies and the underlying matter distribution. The successful tests presented in this work demonstrate the validity of the equations of Perturbation Theory that form a basis for the estimates of Ω which are based on the statistical properties of the velocity divergence field. Their unbiased nature finds its origin in the fact that the relations between the various statistical moments

do not contain any explicit dependence on a bias between the galaxy and the matter distribution. Moreover, the estimated values of Ω are even more direct and straightforward to interpret as the relevant statistical relations only involve a very weak dependence on the cosmological constant Λ is expected to be very weak (Bernardeau 1994a, b).

Not only relations between the statistical moments of the θ distribution, also the shape and general functional behaviour provide a useful indicator for the value of Ω . When we focus on the details of this functional behaviour of the velocity divergence distribution function – illustrated in Fig. 2 and 3) – we can draw a few conclusions with regards the practical feasibility of obtaining reliable estimates from the shape of $p(\theta)$. Both location and shape of the peak of this distribution appear to be robust indicators of the value of Ω . On the other hand, the location of the maximum of the divergence θ – i.e. the cutoff value of $p(\theta)$ – appears to be much more sensitive to a poor sampling. This may make it harder for it to provide reliable estimates of Ω from currently available observational catalogues (see Fig. 3). However, it is all the more encouraging that even on the basis of the cutoff value we obtained a reasonable agreement between theoretical predictions and numerical measurements.

Finally, we addressed one further crucial issue towards an application of our estimation procedures to real data sets. This concerns the problem of not being able to obtain directly the full three-dimensional velocity field. Instead, the velocity of a galaxy can only be measured along the line-of-sight. In a preliminary attempt to study the consequences of this fact for the feasibility of our method, we introduced a partially empirically defined extension of our method. Despite of the extreme crudeness and rather ad-hoc nature of this algorithm to reconstruct the full velocity field, it is quite encouraging that we are able to distinguish between the velocity PDF obtained in a flat Universe and that obtained in an open Universe. The major obstacle towards a successful application of our methods therefore appears to be the one of noisy data sets and systematic sampling errors. We

have not yet dealt with these problems, deferring them to a forthcoming paper.

An additional and useful application of our numerical work involves a test for structure indeed having emerged through the process of gravitational growth of an initially Gaussian random density and velocity field. Having shown Perturbation Theory to be valid, we can exploit its prediction that the PDF of θ is only dependent on a few parameters, in particular σ_θ and Ω . If no values of σ_θ and Ω can be found to produce an acceptable fit to the observed velocity field, this will force us to conclude that it is unlikely that the structure developed as described within the standard framework of gravitational instability and Gaussian initial conditions. In this context it is interesting to point out that a negative skewness has been observed in the currently available datasets (Bernardeau et al. 1995), which is an indication in favour of standard scenarios.

Summarizing, we may conclude that the combined machinery of the analytical perturbation theory results and the developed numerical methods and their application on the intrinsic statistical properties of the velocity field provides us with a reliable new estimator of the cosmological density parameter Ω . This estimator is all the more useful as it is one of the very few which will yield values of Ω completely independent of galaxy-density field biases and almost independent of the value of Λ .

ACKNOWLEDGMENTS

F. Bernardeau would like to thank IAP, where a large part of the work has been completed, for its warm hospitality. We would like to thank A. Dekel for encouraging comments and discussions. FB and RvdW are grateful for the hospitality of the Hebrew University of Jerusalem, where the last part of this contribution was finished.

R. van de Weygaert is supported by a fellowship of the Royal Netherlands Academy of Arts and Sciences. Part of this work was done while EH was at the Institut d'Astrophysique de Paris (CNRS), supported by the Ministère de la Recherche et de la Technologie. Additional partial support to EH was provided by the Danish National Research Foundation through the establishment of the Theoretical Astrophysics Center. The computational means were made available to us thanks to the scientific council of the Institut du Développement et des Ressources en Informatique Scientifique (IDRIS).

REFERENCES

- Bernardeau, F., 1992, ApJ, 292, 1
 Bernardeau, F., 1994a, ApJ, 433, 1
 Bernardeau, F., 1994b, A&A, 291, 697
 Bernardeau, F., Kofman, L. 1995, ApJ, 443, 479
 Bernardeau, F., Juszkiewicz, R., Dekel, A. & Bouchet F., 1995, MNRAS, 274, 20
 Bernardeau, F. & van de Weygaert, R. 1996, MNRAS, 279, 693
 Bertschinger, E., Dekel, A., 1989, ApJ, 336, L5
 Bertschinger, E., Dekel, A., Faber, S.M., Dressler, A., & Burstein, D., 1990, ApJ, 364, 370
 Bouchet, F., Juszkiewicz, R., Colombi, S. & Pellat, R., 1992, ApJ, 394, L5

- Burstein D., Davies R.L., Dressler A., Faber S.M., Stone R.P.S., Lynden-Bell D., Terlevich R.J., Wegner G.A., 1987, ApJS, 64, 601
 Dekel, A., Bertschinger, E., Faber, S.M., 1990, ApJ, 364, 349
 Dekel, A., 1994, ARAA, 32, 371
 Dekel, A., Rees, M.J., 1987, Nature, 326, 455
 Dekel, A., Rees, M.J., 1994, ApJ, 422, L1
 Delaunay, B.V., 1934, Bull. Acad. Sci. (VII) Classe Sci. Mat., 793
 Juszkiewicz, R., Weinberg, D. H., Amsterdamski, P., Chodorowski, M. & Bouchet, F., 1995, ApJ, 442, 39
 Nusser, A. & Dekel, A., 1993, ApJ, 405, 437
 Peebles, P.J.E., 1980, The Large Scale Structure of the Universe, Princeton University Press, Princeton, N.J., USA
 Rubin V.C., Thonnard N., Ford W.K., Roberts M.S., 1976, AJ, 81, 719
 Strauss, M. A., Willick, J. A. 1995, Physics Rep., 261, 271
 Van de Weygaert, R. 1991, Voids and the Geometry of Large Scale Structure, Ph.D. thesis Leiden University
 Van de Weygaert, R. 1994, A&A 283, 361
 Voronoi, G., 1908, J. reine angew. Math., 134, 198

APPENDIX A: CALCULATION OF THE PROBABILITY DISTRIBUTION FUNCTION OF θ

In the case of a top-hat window function it is possible to evaluate the whole series of cumulants of θ at their leading order. This makes it feasible to construct, at least in principle, the complete PDF of the local top-hat smoothed velocity divergence field. However, in order to construct a convenient closed form of the PDF we to introduce some approximations. Here we will go through some of the analytical results and applied approximations that were used in order to obtain simplified final expressions.

A key element in the construction of the PDF of θ is the moment generating function φ_θ and the close relation that was discovered to exist (see e.g. Bernardeau 1992) between this function and the dynamics of spherical collapse in the background Friedmann-Robertson-Walker universe. More specifically, the generating function $\varphi_\theta(\Omega, y)$, defined as

$$\varphi_\theta(\Omega, y) = \sum_{p=2}^{\infty} -T_p(\Omega) \frac{(-y)^p}{p!}, \quad (\text{A1})$$

where T_p are the reduced cumulants of θ introduced in (8), is determined from a function $\mathcal{G}_\theta(\Omega, \tau)$ whose behavior can be deduced from spherical collapse dynamics in the cosmology under consideration. These two functions $\varphi_\theta(\Omega, y)$ and $\mathcal{G}_\theta(\Omega, \tau)$ are related through the system of equations

$$\varphi_\theta(\Omega, y) = y\mathcal{G}_\theta(\Omega, \tau) - \frac{1}{2}y\tau \frac{d}{d\tau}\mathcal{G}_\theta(\Omega, \tau), \quad (\text{A2})$$

$$\tau = -y \frac{d}{d\tau}\mathcal{G}_\theta(\Omega, \tau). \quad (\text{A3})$$

For the solution of this system it is therefore necessary to first determine the explicit relationship of $\mathcal{G}_\theta(\Omega, \tau)$ to the dynamics of spherical collapse. In order to accomplish this, it is useful to introduce the functions $\mathcal{G}_\delta^{SC}(\tau)$ and $\mathcal{G}_\theta^{SC}[\Omega(a), f(\Omega, \Lambda)\tau]$. The first one of these, $\mathcal{G}_\delta^{SC}(\tau)$, is defined to be the nonlinear density contrast of a spherical perturbation of initial over-density $-\tau$. For exact analytical expressions for \mathcal{G}_δ^{SC} , which exist only if $\Lambda = 0$, we refer to appropriate textbooks. Directly related to the expression

for the density contrast is the function describing the local departure from the Hubble expansion,

$$\mathcal{G}_\theta^{SC}[\Omega(a), f(\Omega, \Lambda)\tau] = -a \frac{d}{da} \mathcal{G}_\delta^{SC}(a, \tau) + f(\Omega, \Lambda) \tau \frac{d}{d\tau} \mathcal{G}_\delta^{SC}(a, \tau) / [1 + \mathcal{G}_\delta^{SC}(a, \tau)]. \quad (\text{A4})$$

After having introduced the above two functions and after having written down their explicit expressions, the generating function $\mathcal{G}_\theta(\tau)$ in equation (11) can be obtained through the solution of the system of equations (Bernardeau 1994b),

$$\begin{aligned} \mathcal{G}_\theta(f(\Omega, \Lambda)\tau) &= \mathcal{G}_\theta^{SC} \left[f(\Omega, \Lambda)\tau \frac{\sigma([1 + \mathcal{G}_\delta(\tau)]^{1/3} R_0)}{\sigma(R_0)} \right]; \\ \mathcal{G}_\delta(\tau) &= \mathcal{G}_\delta^{SC} \left[\tau \frac{\sigma([1 + \mathcal{G}_\delta(\tau)]^{1/3} R_0)}{\sigma(R_0)} \right]. \end{aligned} \quad (\text{A5})$$

In principle, the above system of equations can be fully solved to get full-fledged expressions for the coefficients T_p , like e.g. the ones for T_3 and T_4

$$T_3(\Omega = 1, \Lambda = 0) = -\frac{26}{7} - \gamma_1, \quad (\text{A6})$$

$$T_4(\Omega = 1, \Lambda = 0) = \frac{12088}{441} + \frac{338}{21}\gamma_1 + \frac{7}{3}\gamma_1^2 + \frac{2}{3}\gamma_2, \quad (\text{A7})$$

where the γ_p are the successive logarithmic derivatives of the variance with the smoothing scale,

$$\gamma_p \equiv \frac{d^p \log \sigma_\theta^2(R)}{d \log^p R}. \quad (\text{A8})$$

For practical purposes, however, it is preferable to define a simplified set of equations that forms a reasonable approximation to the original system. Several useful approximations can be applied. The first one is to assume that the power spectrum of the density and velocity fluctuations can be accurately described by a power law,

$$P(k) \propto k^n, \quad \sigma^2(R) \propto R^{-(n+3)}, \quad (\text{A9})$$

leading to $\gamma_1 = -(n+3)$ and $\gamma_2 = 0$ in Eqs. (A6) and (A7). Although this may not be exact in general, it may be justified by the fact that we saw previously that the corrections in the values of T_3 and T_4 induced by a variation of the index n enter only weakly.

A second approximation exploits the fact that the Ω dependence of $\mathcal{G}_\delta^{SC}(\tau)$ is extremely weak (see Bouchet et al. 1992, Bernardeau 1992). This implies that equation (A4) reduces to

$$\mathcal{G}_\theta^{SC}[f(\Omega, \Lambda)\tau] \approx -\Omega^{0.6} \tau \frac{d}{d\tau} \mathcal{G}_\delta^{SC}(\tau) / [1 + \mathcal{G}_\delta^{SC}(\tau)]. \quad (\text{A10})$$

Moreover, it is therefore also reasonable to approximate the function $\mathcal{G}_\delta^{SC}(\tau)$, independent of the value of Ω involved, by the simple expression for $\mathcal{G}_\delta^{SC}(\tau)$ for the case $\Omega = 0$,

$$\mathcal{G}_\delta^{SC}(\tau) \approx \left(1 + \frac{2\tau}{3}\right)^{-3/2} - 1, \quad (\text{A11})$$

so that equation (A4), via equation (A10), lead to the approximate relationship

$$\mathcal{G}_\theta^{SC}(\tau) \approx \tau \left(1 + \frac{2\tau}{3\Omega^{0.6}}\right)^{-1}. \quad (\text{A12})$$

Using the above approximate expressions in solving the system of equations in (A3) then yields an approximate expression for the relation between the spherical collapse density contrast τ and the functions $\mathcal{G}_\delta^{SC}(\tau)$ and $\mathcal{G}_\theta^{SC}(\tau)$,

$$\tau \approx \frac{3}{2} (1 + \mathcal{G}_\delta)^{(n+3)/6} [(1 + \mathcal{G}_\delta)^{-2/3} - 1], \quad (\text{A13})$$

and

$$\tau \approx \frac{3}{2} \left(1 - \frac{2\mathcal{G}_\theta}{3f(\Omega)}\right)^{(n+3)/6} \left[\left(1 - \frac{2\mathcal{G}_\theta}{3f(\Omega)}\right)^{-1} - 1\right]. \quad (\text{A14})$$

While reasonable, these approximations turn out not to be as good for the velocity field as for the density field. For example, using the approximations (A11) and (A12) one would obtain $S_3 \equiv \langle \delta^3 \rangle / \langle \delta^2 \rangle^2 = 5 - (n+3)$ instead of $S_3 = 34/7 - (n+3)$, and $T_3 = -4 + (n+3)$ instead of $T_3 = -26/7 + (n+3)$. This means that for example for $n = -1$ the relative errors in S_3 and T_3 are in the order of 5% and 15%.

While the above expose explains the strategy for calculating the coefficients T_p to any order, the major purpose of calculating the generating function (11) is to construct the PDF of the local velocity divergence. This is achieved through a Laplace inverse transform (Balian & Schaeffer 1989),

$$p(\theta)d\theta = \int_{-i\infty}^{+i\infty} \frac{dy}{2\pi i \sigma_\theta^2} \exp\left[-\frac{\varphi_\theta(y)}{\sigma_\theta^2} + \frac{y\theta}{\sigma_\theta^2}\right] d\theta, \quad (\text{A15})$$

where σ_θ is the variance of the distribution. The saddle point approximation of this integral

$$\begin{aligned} p_\theta(\theta)d\theta &= -\frac{1}{\mathcal{G}'_\theta(\tau)} \left[\frac{1 - \tau \mathcal{G}''_\theta(\tau) / \mathcal{G}'_\theta(\tau)}{2\pi\sigma_\theta^2} \right]^{1/2} \\ &\times \exp\left(-\frac{\tau^2}{2\sigma_\theta^2}\right) d\theta, \quad \mathcal{G}_\theta(\tau) = \theta, \end{aligned} \quad (\text{A16})$$

yields an accurate prescription for the shape of PDF, in particular around its maximum (see Bernardeau 1994b for more details).

By subsequently invoking the approximate expressions (A11) and (A12), and using the fact that then equations (A13) and (A14) can be inverted, one can find simple analytic fits [Eq. (12)] for the special case of $n = -1$.

APPENDIX B: θ FROM ONE VELOCITY COMPONENT: AN ILLUSTRATIVE EXAMPLE

It is possible to estimate the bias μ and the variance of the noise σ_e involved in our calculation of θ [Eq. (18, 19)] with the simple following model: let us assume that the difference of velocity between two given neighboring points is collinear to their relative position $\Delta \mathbf{r}$

$$\Delta \mathbf{v} = \Theta \frac{\Delta \mathbf{r}}{\Delta r}, \quad (\text{B1})$$

leading to $\theta_{\text{wall}} = \Theta$. This assumption is generally not true, even for an irrotational flow, because it overlooks any possible shear. However this should be enough for a rough estimation of μ and σ_e , and to show that they do not depend directly on Ω . Considering that only the velocity along the direction x is known, our estimate of the divergence [Eq. (18)] yields

$$\theta_{\text{wall}}^{\text{estim.}} = \Delta v_x \frac{n_x}{n_x^2 + \epsilon} = \Theta \frac{n_x^2}{n_x^2 + \epsilon}. \quad (\text{B2})$$

If we now assume that the direction of $\Delta \mathbf{r}$ is randomly distributed in a 3 dimensional space, the bias is, according to our empirical parametrisation (19), (the subscript “wall” of θ will be dropped hereafter)

$$\mu = \frac{\langle \theta_{\text{estim.}} \theta \rangle}{\Theta^2} = \left\langle \frac{n_x^2}{n_x^2 + \epsilon} \right\rangle = 1 - \sqrt{\epsilon} \arctan(\epsilon^{-1/2}). \quad (\text{B3})$$

This implies that the noise

$$e = \Theta \left(\frac{n_x^2}{\mu(n_x^2 + \epsilon)} - 1 \right) \quad (\text{B4})$$

has a vanishing average, and its variance is

$$\begin{aligned} \sigma_e^2 &= \Theta^2 \left[\frac{1}{\mu^2} \left\langle \frac{n_x^4}{(n_x^2 + \epsilon)^2} \right\rangle - 1 \right] \\ &= \frac{\Theta^2}{\mu^2} \left[1 + \frac{\epsilon}{2(1 + \epsilon)} - \frac{3\sqrt{\epsilon}}{2} \arctan(\epsilon^{-1/2}) - \mu^2 \right] \end{aligned} \quad (\text{B5})$$

with $0 \leq \sigma_e^2 \leq 0.562 \Theta^2$ for $0 \leq \epsilon \leq 1$.

We can now assume that Θ is itself a random variable *independent* of n_x such that $\langle \Theta \rangle = \langle \theta \rangle = 0$ and its variance $\langle \Theta^2 \rangle = \sigma_\theta^2$ is given in Table 1. This variance does not have an explicit dependence on Ω , and therefore σ_e does not, while it does depend on the evolutionary stage of the system and the scale that is considered. On the other hand, μ is clearly completely independent of Ω . Analytical results for the bias and the noise are given in Table 3 and can be compared to their respective numerical values listed in Table 2.

Taking this model at face value would tell us to put $\epsilon = 0$ giving $\mu = 1$ and $e = 1$, i.e. $\theta_{\text{estim.}}$ would be a perfect estimator of θ . This is of course not true because of the neglected shear component and of the vorticity likely to be present at small scale, not to mention the instability of such a numerical estimate. However, in spite of its extreme crudeness, this model gives fairly good analytical predictions of the ‘intrinsic’ bias and noise introduced by our numerical estimates of the velocity divergence, and indicates that the remaining noise due to shear and vorticity is almost negligible.